MANSOURA JOURNAL OF Physics
Official Journal of Faculty of Science, Mansoura University, Egypt
E-mail: scimag@mans.edu.eg ISSN: 2974-4954

Influence of Sb on microstructure, elastic properties and radiation shielding properties of rapidly solidified Sn-Bi lead-free shielding alloys to be used in radiotherapy applications.

Borkan Abdulaziz Al-Rawe[a,b], Nermin Abdelhakim[a], S. Salama[c],, Rizk Mostafa Shalaby[a,]

[a] *Material Physics Research group, Physics Department, faculty of Science, Mansoura University, Mansoura, Egypt*

[b] *on leave, M.Sc. student, Ministry of Higher Education, Iraq.*

[c] *Radiation protection &Civil Defense department, nuclear research Center, Atomic energy authority, PO.13759. Cairo, Egypt*

**Corresponding author: email: rizk2002@mans.edu.eg Tel.,: 01062507736*

Received:29/5/2023
Accepted:13/6/2023

Abstract: Because the harmful effects and toxicity on human organs as well as the different environmental drawbacks are devastating. Thus, we need to find sustainable radiation shielding alloy to protect the environment and workers in medical fields from destructive impact of harmful radiation. So, in this present work, five based lead-free radiation shielding alloys doped with semimetal Sb element are prepared by rapid solidification processing technology using melt-spun technique. The different five alloys named are based on chemical composition formula Sn-Bi-Sb_x [x=0, 2.0, 4.0, 6.0 and 8.0 wt.%]. The shielding attenuation properties are measured using FH 40 G dose rate measuring unit. The calculated linear attenuation coefficient LAC μ_l,, mass attenuation coefficient MAC μ_m, half-value layer HVL, tenth-value layer TVL, mean free path MFP, are performed theoretically by using Phy-X/PSD computer programs in the energy range from 15 keV to 15 MeV. A correlation study was conducted to find the optimum shielding parameters for the fabricated shielding alloys. The structure, microstructure features, and mechanical properties of the prepared shielding alloys were characterized and analyzed. The phase identification and morphology of the shielding alloys were studied using X-ray diffraction and scanning electron microscopy. The structural analysis indicated that crystallite size was reduced by increasing Sb content in the Sn matrix which enhances the elastic constants of radiation shielding materials. The Bi_{50}-Sn_{50} binary alloy composition is reported to exhibit maximum shielding efficiency. This current study focused on the study and development of new lead-free radiation shielding alloys in nuclear medicine. Results from this study show that these metallic alloys are very useful for gamma ray shielding and the best candidate for lead-based shielding material

Keywords: rapid solidification processing; environmentally friendly alloys; new candidate lead-free shielding; radiotherapy applications

1. Introduction

The biological shields are defined as the radiation protection shielding which reduce the time and radiation exposure of workers in hospitals and nuclear reactors places. Also to protect sensitive electronic devices are used in nuclear reactors places in the field of radiation. So, to protect important military devices and electronic devices which found in laboratories and within the nuclear r perimeter [1-4]. A lot of researchers dioscovered the a useful shielding of radiation preservation such as ceramics, concrete, metallic alloys and glasses [5-9]. Rencently, some binary systems such as Pb-Sn, Pb-Zn and Sn-Zn are studied by Sharma

et al. [10]. Different alloys as gamma rays shielding material has been analyzed by different researchers : brarss, bronze, steel, Al-Si, Pb-Sb were discovered by El-Kateb et al. [11] ; nickel and vanadium metallic materials were studied by Singh et al. [12] ; binary alloys of Ti-Ni and Ni-Cr were studied by Han and Demir [13,14]; Cu-Pb alloys were studied by Singh et al. [15], binary alloys of Pb-Sn, Pb-Zn and Sn-Zn alloys by Sharma et al. [16]. The binary alloys of Pb-Sn in different compositions were selected for the present work with a stimulus to decrease the poisoining of Pb element with tin, wiithout much compensation in the effectiveness towards photon absorption. Sharma et al. [16], has been made to visualize the scope of some binary alloys of Pb-Sn as radiation shielding material. The affirmation has been focused on the dependence of exposure buiildup factor on the incident energy, peenetration depth and chemical composition of the prepared alloy samples. Reecently, [17-19] investigated the rradiation sshielding performance of lead-free Sn-Zn-Bi binary and ternary alloys. Ammong various alloys, the Sn-Zn-Bi-Pb binary and tternary alloys have received a great attention in physical and raddiation attenuation because of steveral benefits such as high density, ease of mannufacturing, strong creep resistance , high joint strength, superior wettability, relatively low cost, efficient mechanical and thermo-physical properties , and corrosion resistance [20-22]. The present work aims to study the impact of Sb on a new fabricated Sn-Bi shielding materials series. Therefore , some of the elastic constants were analyzed. Furthermore, the shielding properties are determined experimentally and theoretically. Also, the ability of the prepared shielding to attenuate the gamma photons with an energy range varied between 15 KeV and 15 MeV was evaluated.

2. General experimental details

2.1 Materials preparation and characterization

The chemical compositions Sn_{50}-Bi_{50-x}-Sb_X (X=2, 4, 6 and 8 wt.%) alloys were fabricate from high purely aluminum, zinc and tin (purity>99.9%). The shieldin g metallic alloys under investigations were fabricated using single wheel of melt-spun- technique. The melt-spun technique was discussed in details early [23, 24]. One of the most important is increasing of solid solubility with increasing cooling rate and consequentely reduce the scale of microstructure which improve the alloy elastic constants as well as segregation and therefore the second phase content [25, 26]. X-ray diffraction using CuKα is used to identify the phase structure and lattice distortion. The elastic constants of prepared alloys were examined using a dynamic resonance technique. Vickers microhardness ttechnique were used to identify the Microhardness tests using a digital Vickers microhardness tester (model FM-7. The microstructures features of as-melt-spun technique of shielding alloys, was studied by scanning electron microscopy (SEM. The detailed chemical composition, experimental density and thickness of the prepared melt-spun alloys are tabulated in tables [1, 2] respectively.

Table 1: The nominal compositions of as prepared melt-spun radiation shielding alloys (wt.%).

Shielding alloy	Composition wt.%			
	Sn	Bi	Sb	
Sn-50Bi	bal	50	–	
Sn-48Bi-2Sb	bal	48	2	
Sn-46Bi-4Sb	bal	46	4	
Sn-44Bi-6Sb	bal	44	6	
Sn-42Bi-8Sb	bal	42	8	

Table 2: measured density of as prepared alloys.

shielding system	experimental density(g/cm^3)	Thickness mm
Sn-50Bi	8.53	0.208
Sn-48Bi-2Sb	8.467	0.143
Sn-46Bi-4Sb	8.405	0.161
Sn-44Bi-6Sb	8.344	0.171
Sn-42Bi-8Sb	8.283	0.173

2.2 Hardness test

Microhardness tests were conducted using a d igital Vickers microhardness tester type -FM-7-Japan), applying a load of 0.098 and 0.245 N was applied for different indentation time (dwell time) [27], where a diamond pyramid indenter with square base

on a smooth surface of the alloy and Vickers hardness number is given by Hv= 0.185F/d^2, where F is the applied load in N and d is the average diagonal le ngth in mm. It was found that this used load is sufficiently small to suppress any tendency to cracking, which can grossly affect the hardness measurements. Fifteen consecutive indentations with standard deviations were performed for each alloy with 20 microns distance between each indent mark. The highest and lowest hardness values were neglected and the remaining thirteen were used in calculations. The average and the standard deviation of thirteen values w ere calculated and tabulated.

2.3 Mechanical properties tests

Melt-spun process Sn_{50}-Bi_{50-x}-Sb_X (X=2.0, 4.0, 6.0 and 8.0 wt.%) materials were characterized using computerized tensile testing machine previously discussed in details [28, 29] at strain rate of 1.25 x 10^{-3} s^{-1}. The stress and strain ($\sigma = F/A$ and $\varepsilon = \Delta l/l$ respectively), where F, is applied force, Δl is change in length and A, the cross-section area . Stress-strain typical curve is drawn automated using computer setting that contains software program to detect the tensile properties.

3 Results and discussion

3.1 Structure analysis (XRD)

XRD analysis for Sn-50-xBi-Sb_x (x =0,2.0, 4.0, 6.0 and 8.0 wt.%) rapidly solidified using melt-spun process at cooling rate 10^5 K/sec are illustrated in Fig.1. The spectrum of all the melt-spun process alloys show the presence of tetragonal β-Sn (PDF 01-085-5862) has I41/amd (141) with a= 5.86 and c= 3.193 A and c/a 0.5449, Rhombohedral Bi(PDF 01-085-5857)), R-3m (166) at hkl (003), (101), (012) and (104) where a= 4.545 and c= 11.9 A and c/a = 2.618 , in the crystalline form in addition rhombohedral R-3m (166) has a= 4.325 and c= 5.346 , and c/a = 1.236, SnSb IMC (Stistaite, syn) (PDF 00-033-0118) was also observed at (101), (012), (110) and (003) . The lattice constants results by XRD for Sn-Bi-Sb of β-Sn phase is tabulated in Table 2. The results of the lattice constants are shown in Table 2, where the variations in the lattice constants of the β-Sn phase increases with Sb addition. Grain size (Å) for prepared alloys reduces with Sb content as displayed in Table 3.

Fig. 1 shows the XRD spectrums for shielding Sn_{50}-Bi_{50-x}-Sb_X (X=2, 4, 6 and 8 wt.%) alloys. The XRD analysis is listed in Table 1. The grain size (D) was derived from the XRD pattern by using Scherrer formula [30].

$$D = \frac{0.9\lambda}{\beta cos\theta} \qquad (1)$$

where θ is the Bragg angle, λ is the wavelength of x-rays, β is (FWHM). The grain size lowering by increasing Sb content in the Sn matrix which enhances the mechanical properties of shielding alloys.

After calculating volume of the unit cell (V) by through the lattice parameters, the number of atom s in the unit cell (n) is calculated using the following equations [31].

$$\Sigma A = \frac{\rho v}{1.66020} \qquad (2)$$

$$\Sigma A = n\, Aw \qquad (3)$$

where ΣA is the sum of the atomic weights of the atoms in the unit cell, ρ is the density (gm/cm^3) and V is the volume of the unit cell (nm^3), and Aw is the molecular mass. The number of atoms per unit cell was calculated which is nonintegral number of atoms per cell. Therefore, some of the atoms may be absent from a sure fraction of those lattice sites, which they would be expected to occupy.

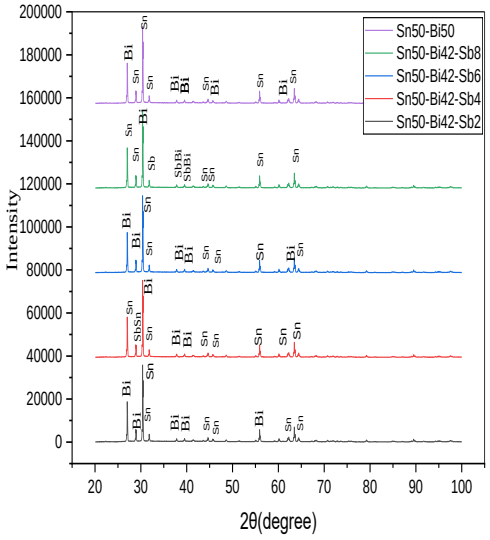

Fig. 1. The XRD patterns of as prepared Sn-Bi-Sb shielding alloys.

Table 3: The details of the XRD analysis of as- prepared Sn-Bi-Sb shielding alloys.

Melt-spun ribbons	Phase designation	Crystal system	Crystallite size D (nm)	No of atoms / unit cell of Sn phase
Sn-50% Bi	Sn	Tetragonal	510.11	4.25
	Bi	Monoclinic		
Sn-48%Bi- 2% Sb	Sn	Tetragonal	480.60	4.44
	Bi	Monoclinic		
	SbSn			
Sn-46%Bi- 4% Sb	Sn	Tetragonal	420.60	4.11
	Bi	Monoclinic		
	SbSn			
Sn-44%Bi- 6% Sb	Sn	Tetragonal	390.33	4.01
	Bi	Monoclinic		
	Sb	Rhombohedral		
Sn-42%Bi- 8% Sb	Sn	Tetragonal	311.78	3.97
	Bi	Monoclinic		
	Sb	Rhombohedral		
	BiSb			

3.2 Microstructure (SEM)

Typical microstructures seen in the Sn_{50}-Bi_{50-x}-Sb_X (X=2, 4, 6 and 8 wt.%) alloys are highly homogenous and include Sn dendrite phase in addition IMCs from reaction between the Sn and alloying elements and different locations in the microstructures. The microstructure representative of homogenous in the free Sb and Sb-containing Sn_{50}-Bi_{50-x}-Sb_X (X=2, 4, 6 and 8 wt.%) alloys are shown in Fig. 2. All the alloys have Sn eutectic dendrites structure tha t forms between the dendrites, and Bi precipitation in the Sn dendrites and Sn in the eutectic during rapid cooling to room temperature..

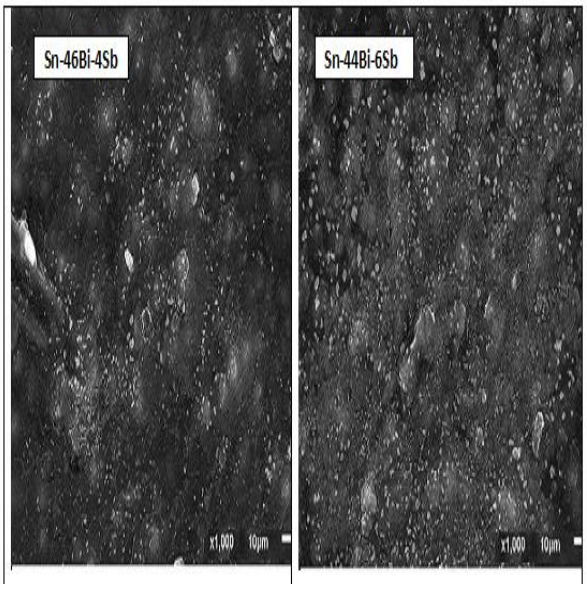

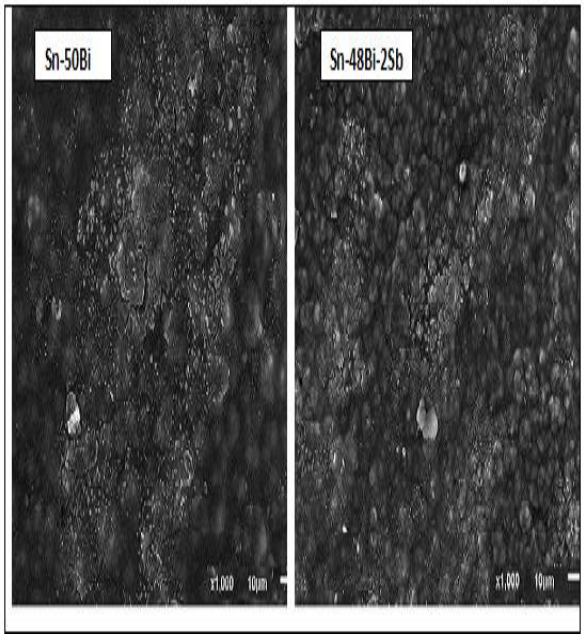

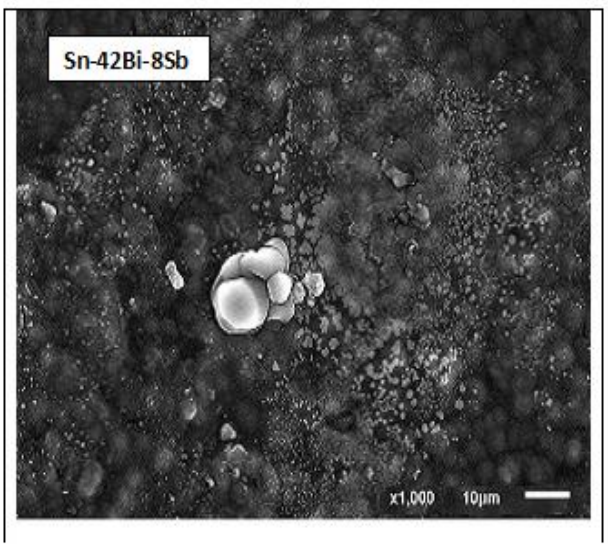

Fig.2: SEM morphology of the constituent phase distribution of all-as prepared melt-spun alloys

3.3 Mechanical Properties

3.3.1 elastic properties

The results of unia xial tensile test for Sn-Bi50-x-Sbx (x = 0, 2, 4, 6, and 8 wt.%) alloys are drawn in Fig.3. The information extracted from the diagrams in Fig.3 is tabulated in Table 4. The stre ngth of Sn -Bi-Sb alloy has a g ood impr ovement compared to Sn-Bi binary alloy. It was also observed that the reduction of its elongation compared to the Sn-Bi is about 100 %. Sn-Bi-Sb alloy toughness and elongation have changed significantly compared to Sn-Bi alloy. As well as its yield stress and UTS have enhanced compared to Sn-Bi. Sn-Bi-8Sb shielding is slightly different from the other four samples related to strength and has a significant improvement in UTS. High elastic strain is produced in these particles and the particles bear a significant part of the total load [32].

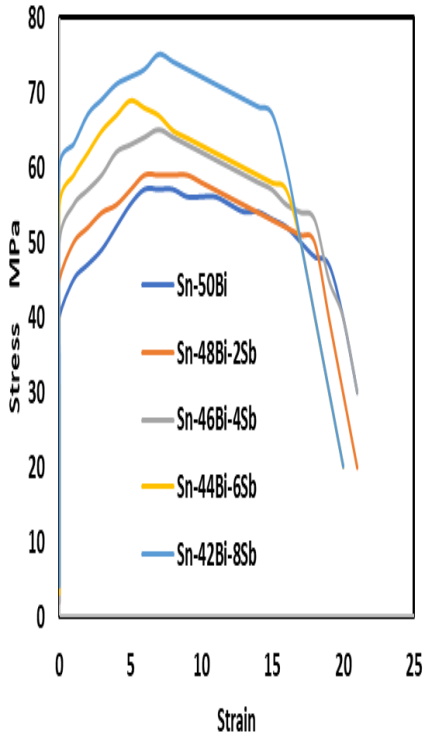

Fig.3: Typical stress-strain curves for all as-prepared melt spun-process alloys

3.3.2 Vickers microhardness changes

The mechanical properties , i.e., the micro hardness (H_V) of the rapidly solidified materials, also depend on the highcooling rate and solidification parameters. However, the mechanical properties of melt-spun process ribbons are usually determined by hardness test. The mechanical behavior was controlled by Vickers hardness testing machine, which is one of t he simplest, suitable, easiest, and most straightforward techniques f or prepared ribbons. Rapidly solidification processing of Sn-50Bi-xSb melt-spun ribbons were t ested for ductility by a simple 180° bending test and checked for brittle fracture. All the melt-spun ribbons exhibited good bending ductility and could be bent through 180° without fracture. In this study, the Vickers micro hardness measurement of melt-spu n ribbons were determined and analyzed. It uses one applied load (0.098 N) to measure the Vickers microhardness values (H_v) of melt-spun ribbons. The values were calculated using the standard Vickers formula: $Hv=2P\sin\theta/2/d^2 = 1.8544P/d^2$, where, P is the indentation force, d is the average diagonal length, and 1.8544 is a geometrical factor for the diamond pyramid. However, to complete the investigation of microstructures, we also measured vickers hardness Hv. The experimental values are tabulated in Table 5. Table 5 shows that the Hv values for all quenched ribbons increased with increasing Sb amount. Furthermore, alloys with the high antimony weight have the highest hardness values. The Hv of quenched ribbons is larger than those of the Sb -free alloy, it is in agree with [33]. Therefore, this high Hv it ios may be due to the lowering in crystallite size. The grain size in quenched Sn-Bi-Sb ribbons is much smaller than the crystallite size in the Sb-free alloy.

Table 4: Elastic properties parameters of all as-prepared melt-spun process alloys

alloy	Young's modulus GPa	Ultimate tensilest rengthMPa	Elongation (%)	Ductility(MJ/m^3)
Sn-50Bi	55.53	57.12	40	3.88
Sn-48Bi-2Sb	58.22	59.10	35	2.19
Sn-46Bi-4Sb	63.54	65.14	27	1.52
Sn-44Bi-6Sb	68.22	69.22	25	1.20
Sn-42Bi-8Sb	75.55	75.23	20	0.57

Table 5: Vickers microhardness values for Sn-Bi -Sb based shielding alloys.

alloy	Hv MPa
Sn-50Bi	320 ± 4.5
Sn-48Bi-2Sb	350 ± 5.6
Sn-46Bi-4Sb	370 ± 4.8
Sn-44Bi-6Sb	380 ± 3.6
Sn-42Bi-8Sb	420 ± 4.2

3.4 Shielding parameters

The linear attenuation coefficients, mass attenuation coefficients (μ/ρ), HVL, TVL and MEP of the five shielding samples at energies between 15 KeV and 15 MeV are measured and estimated as provided in Fig.4 and table.6. Fig.4 shows a result of variation of mass attenuation , linear attenuation coefficient (in cm), half-value layer HVL, tenth-value layer TVL, and mean free path MFP with photon energy in a range of 0.015–15 MeV for all prepare d alloys. The Fig.4 shows that Sn-42Bi-8Sb alloy has the largest attenuation value, followed by Sn-44Bi-6Sb, Sn-46Bi-4Sn, Sn-48Bi-2Sb, and the lowest attenuation value was the Sn-50Bi alloy. It can be concluded that lead-free Sn-42Bi-8Sb alloy is a superior gamma radiation shielding alloy that offers identical shielding effect to Tin - bismuth based alloys doped with Sb. Therefore, lead-free doped 8Sb element with higher attenuation value is considered to be another suitable material for gamma radiation shielding. Therefore, the obtained results show that mass and linear attenuation coefficient increases with the increase in the Sb weight percentage. A comparative study was conducted on radiation shielding properties of antimony-free alloy and alloys doped with Sb. Results from this study show that thes e metallic a lloys are very useful for gamma ray shielding and the best candidate for lead-free shielding material.

Table 6.1: Exp. Shielding properties for Sn-50Bi

Radiation source	DR_{0s}μSv/h	DR_{0s}μSv/h
Cs-137	3.2	3.5
Co-60(1)	3.7	3.9
Co-60(2)	67	72
Co-60(3)	72	80

Table 6.: Exp. Shielding properties for Sn-48Bi- **2**Sb

Radiation source	DR_{0s}μSv/h	DR_{0s}μSv/h
Cs-137	3.1	3.6
Co-60(1)	3.8	4.1
Co-60(2)	69	72
Co-60(3)	74	82

Table 6.3: Exp. Shielding for properties Sn-46Bi- 4 Sb

Radiation source	DR_{0s}μSv/h	DR_{0s}μSv/h
Cs-137	3.3	3.8
Co-60(1)	3.9	4.2
Co-60(2)	69	75
Co-60(3)	75	84

Table 6.4: Exp. Shielding for properties Sn-44Bi- 6 Sb

Radiationsource	DR_{0s}μSv/h	DR_{0s}μSv/h
Cs-137	4.15	4.25
Co-60(1)	3.5	3.6
Co-60(2)	69	70
Co-60(3)	93	92

Table 6.5: Exp. Shielding for properties Sn-42Bi- 8 Sb

Radiationsource	DR_{0s}μSv/h	DR_{0s}μSv/h
Cs-137	3.3	3.85
Co-60(1)	3.18	3.38
Co-60(2)	71	67
Co-60(3)	80	73

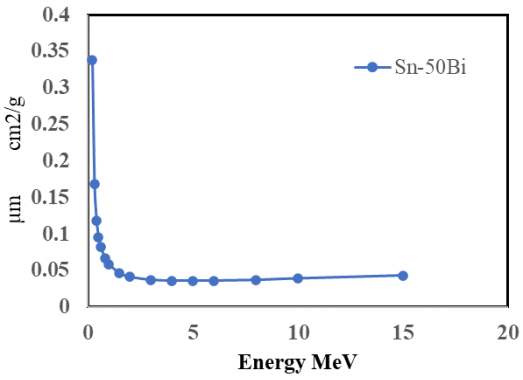

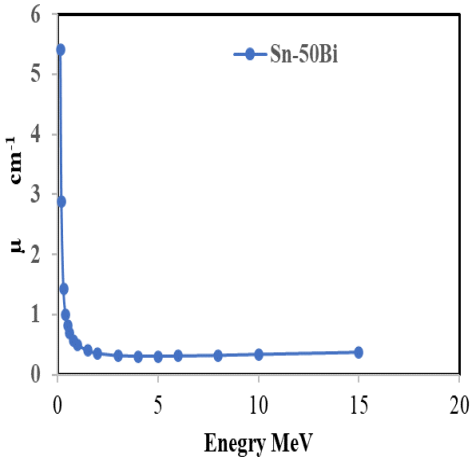

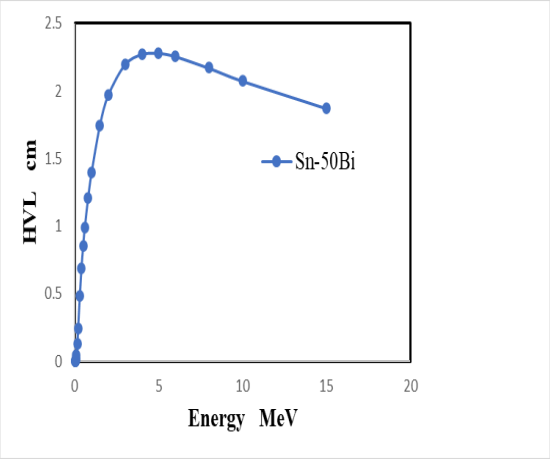

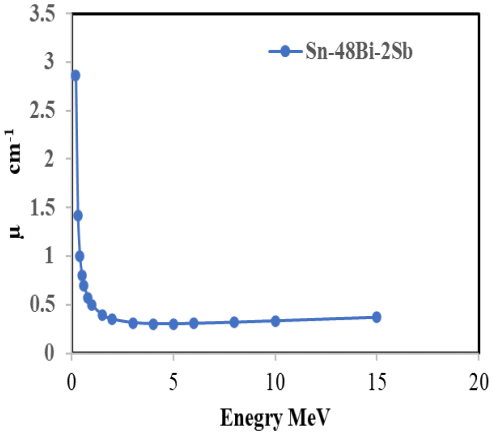

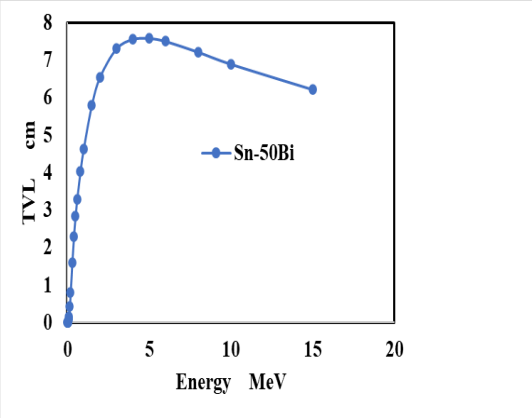

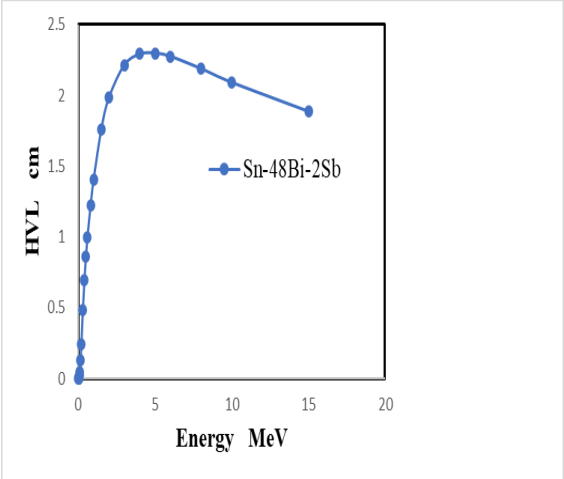

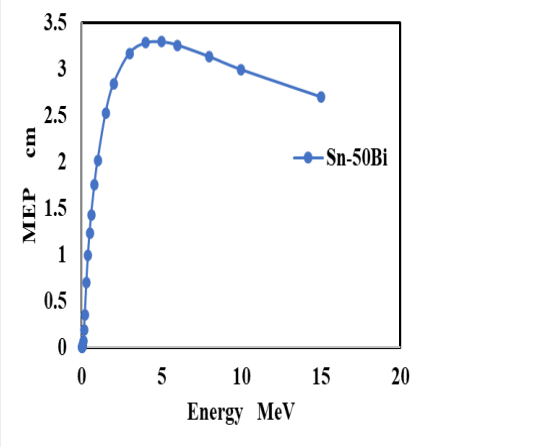

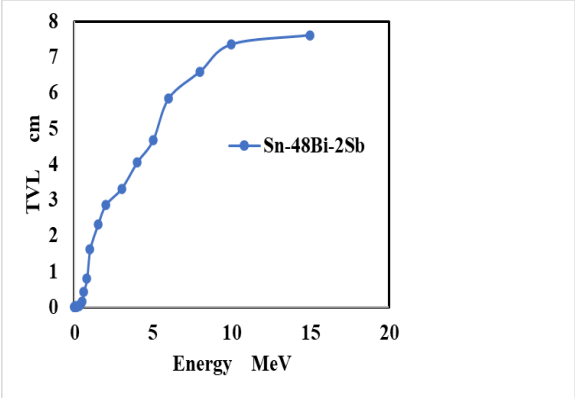

Shielding properties for sample 1

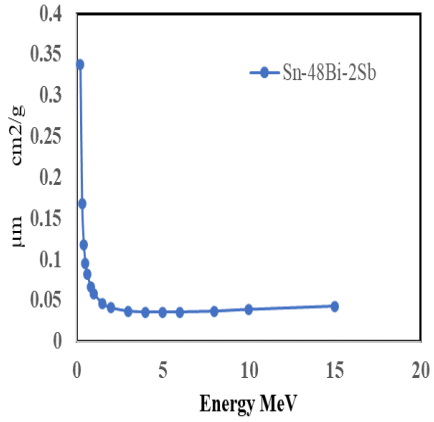

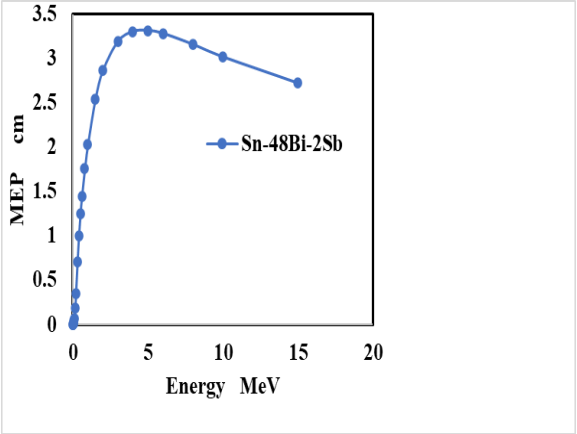

Shielding properties for sample2

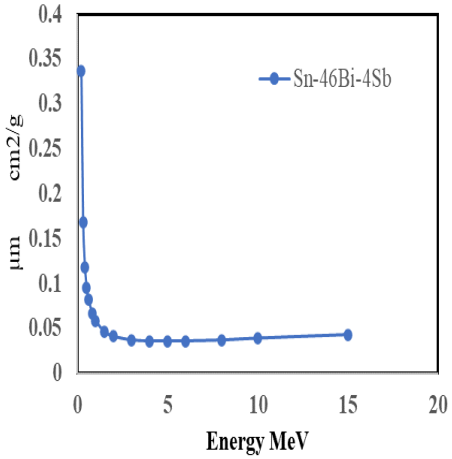

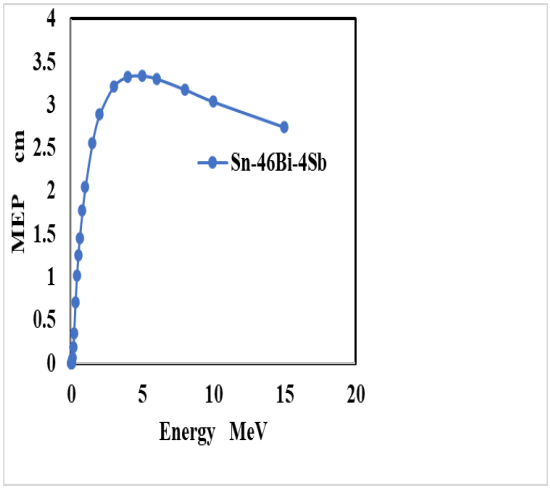

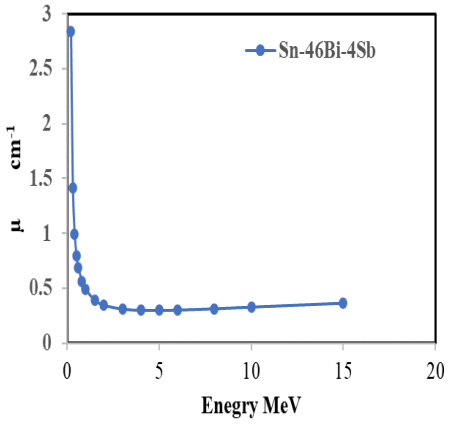

Shielding properties for sample3

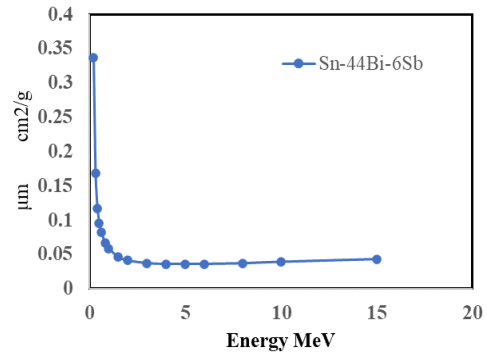

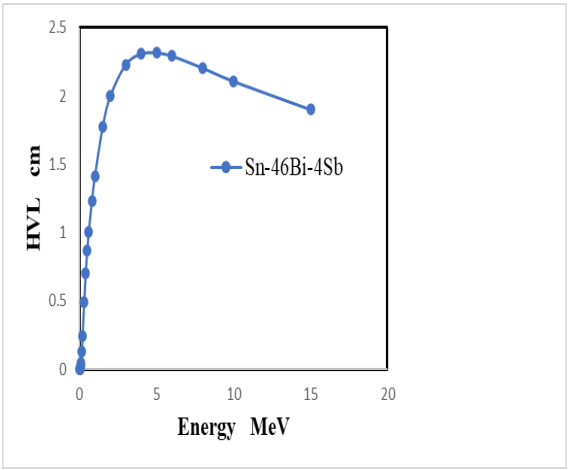

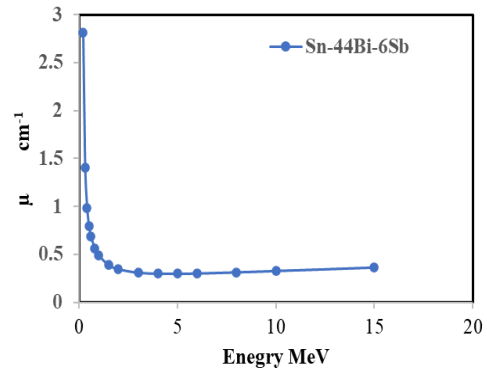

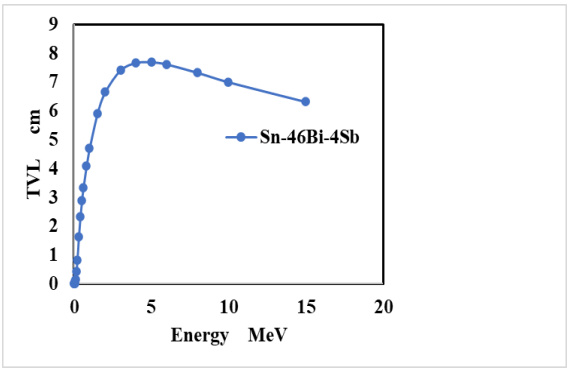

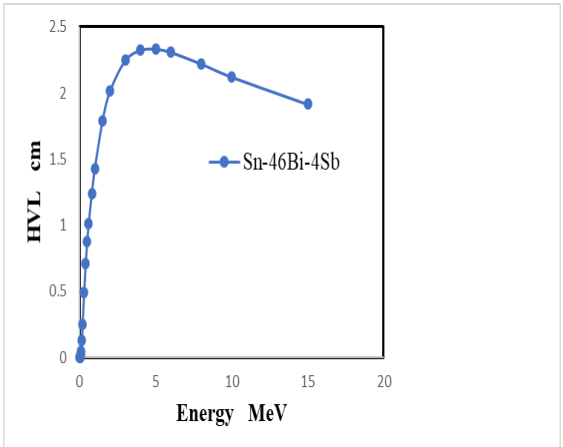

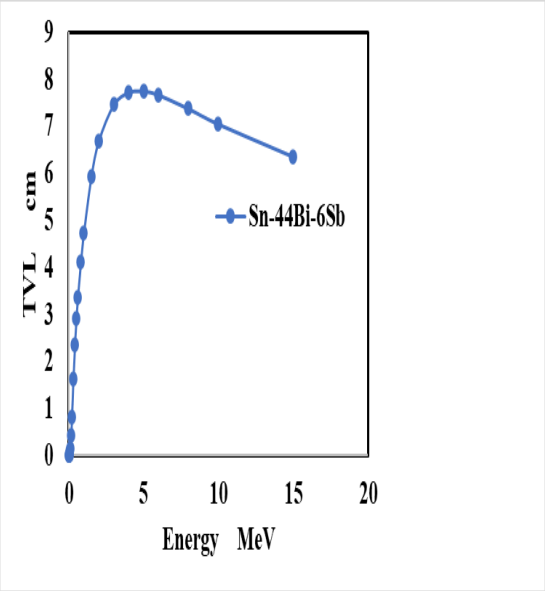

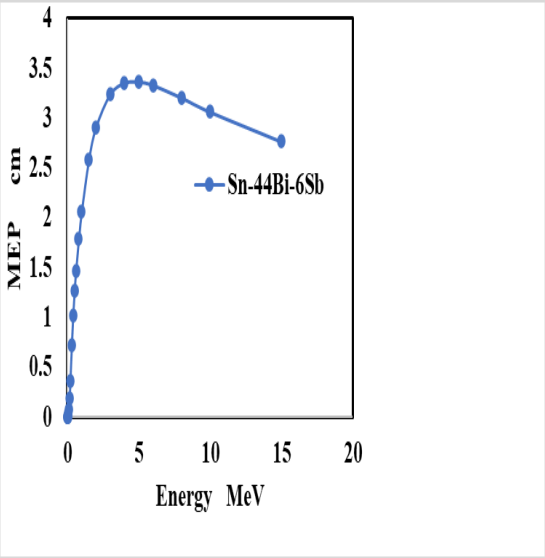

Shielding properties for sample4

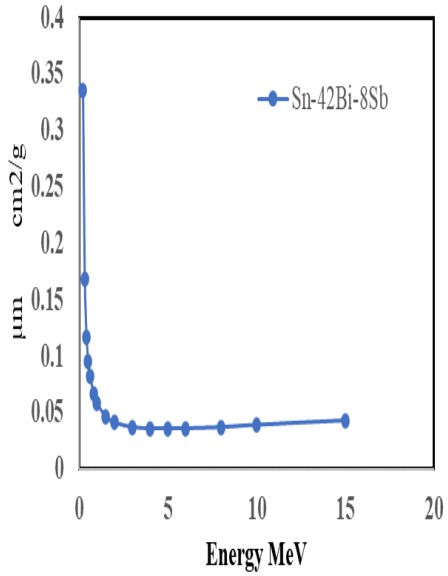

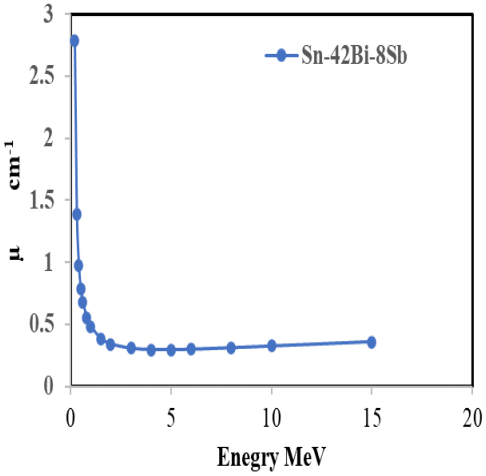

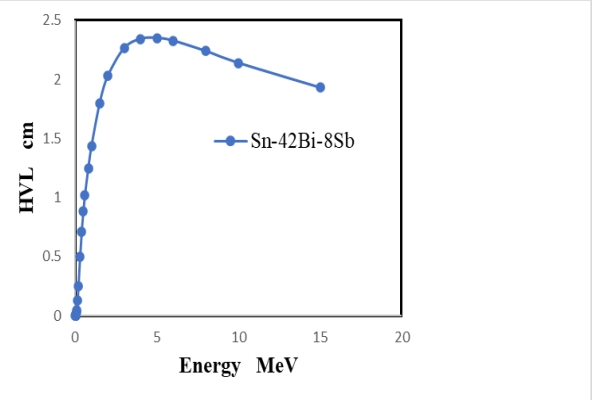

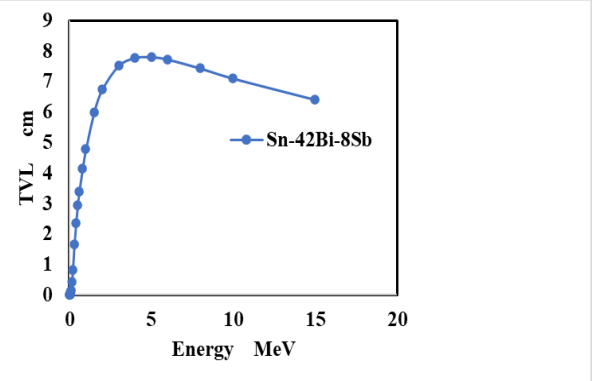

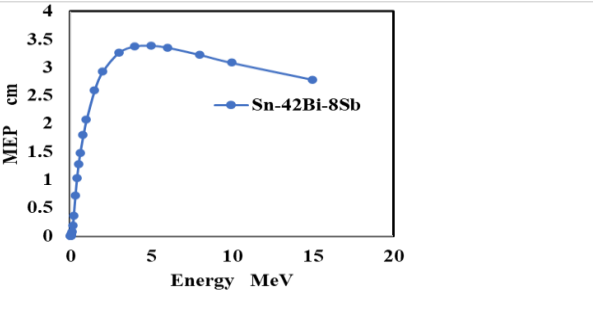

Shielding properties for sample5

Fig.4: The shielding parameters for all prepared samples

Conclusions

The present work investigated a different composition of Sn-Bi-Sb_x (x = 0.0, 2.0., 4.0 6.0 and 8.0 wt.%) binary and ternary alloys to be used as shielding metallic alloys against gamma-rays in the field of nuclear radiation. Also, the influence of increasing Sb addition on the structure, elastic properties, and radiation shielding performances of Sn-Bi-Sb alloys has been analyzed. The followingconclusions can be drawn as:

1. X-ray diffraction revealed that the presence of both β-Sn tetragonal, Bi monoclinic inaddition to IMCs SnSb and BiSb as hard inclusions I n a soft matrix of Sn-based solidsolution and extension of solid solubility of Bi in Sn.

2. Elastic moduli and Vickers microhardness are improved by reducing the crystallite size after the addition of Sb element.

3. In S4 and S5 after Sb amount is increased , it is noticed that the no. of SnSb and BiSb fined particles increased and the β-Sn grains is much coarsened, which leads to a considerable increase in ductility) and mechanical strength.

4. It is also found that the shieldingparameters such as MAC μ_m, LAC μ_l, half-value layer HVL, tenth-value layer TVL, mean free path MFP of all melt-spun alloys are dependent on the elemental composition as well as the energy of the inciden t photons

5. The study clarified that the prepared s amples have a hig h ability to attenuate gamma rays compared to lead as a standard shielding material.

References

1 Sayyed, M. I. et al. (2020) Oxyfluoro-tellurite-zinc glasses and the nuclear-shielding ability under the substitution of AlF3 by ZnO. Appl. Phys. A Mater. Sci. Process. 126, 88.

2 Kaewjaeng, S. et al. (2019). High transparency La2O3-CaO-B2O3-SiO2 glass for diagnosis X-rays shielding material application. Radiat. Phys. Chem. **160**, 41–47

3 Şakar, E., Akbaba, U., Zukowski, E. & Gürol, A. (2018). Gamma and neutron radiation effect on Compton profile of the multi-walled carbon nanotubes. Nucl. Instrum. Methods Phys. Res., Sect. B **437**, 20–26

4 Araz, A., Kavaz, E. & Durak, R. (2021). Neutron and photon shielding competences of aluminum open-cell foams filled with different epoxy mixtures: An experimental study. Radiat. Phys. Chem. **182**, 109382

5 Kaewjang, S. et al. (2014). New gadolinium based glasses for gamma-rays shielding materials. Nucl. Eng. Des. **280**, 21–26

6 Levet, A., Kavaz, E. & Özdemir, Y. An (2020). experimental study on the investigation of nuclear radiation shielding characteristics in iron-boron alloys. *J. Alloys Compd*. 819, 152946

7 Mansy, M. S., Lasheen, Y. F., Breky, M. M. E. & Selim, Y. (2021) Experimental and theoretical investigation of Pb–Sb alloys as a gamma radiation shielding material. Radiat. Phys. Chem. **183**, 109416.

8 Sayyed, M. I. et al. (2021). Radiation shielding characteristics of selected ceramics using the EPICS2017 library. Ceram. Int. **47**, 13181– 13186

9 Sayyed, M. I., Olarinoye, O. I. & Elsaf, M. (2021). Assessment of gamma-radiation attenuation characteristics of Bi2O3–B2O3–SiO2–Na2O glasses using Geant4 simulation code M. Eur. *Phys. J. Plus* **136**, 535

10 Sharma, R., Sharma, J.K., Singh, T., (2016) Effective atomic numbers for some alloys at 662 keV using gamma rays backscattering technique. *Phys. Sci. Int. J.* **11 (1),** 1-6.

11 El-Kateb, A.H., Rizk, R.A.M., Abdul-Kader, A.M., (2000) Determination of atomic cross-sections and effective atomic numbers for some alloys. Ann. Nucl. Energy 27,**14**, 1333-1343.

12 Singh, T., Kaur, P., Singh, P.S., (2006) Parameters of dosimetric interest of some vanadium and nickel compounds. *Asian J. Chem.* **18**, 3325e3328.

13 Han, I., Demir, L., (2009), Studies on effective atomic number, electron density from mass attenuation coefficients in TixCo1-x and CoxCu1-x alloys. Nuclear Instruments and Methods in Physics

Research Section B: Beam Interactions with Materials and Atoms, V.**267**, Issue.21-22, 3505-3510.

14 Han, I., Demir, L., (2009) Mass attenuation coefficients, effective atomic and electron numbers of Ti and Ni alloys. Radiat. Meas. **44,** , 289-294.

15 Singh, T., Kaur, S., Kaur, P., Kaur, H., Singh, P.S., ,(2015) Variation of photon interaction parameters with energy for some Cu-Pb alloys. AIP Conference Proceedings 1675020057; https://doi.org/10.1063/1.4929215

16 Sharma, R., Sharma, J.K., Singh, T., (2016) Effective atomic numbers for some alloys at 662 keV using gamma rays backscattering technique. *Phys. Sci. Int. J.* **11 (1)**, 1-6.

17 A. Saleh, Rizk Mostafa Shalaby, Nermin Ali Abdelhakim, (2022) Comprehensive study on structure, mechanical and nuclear shielding properties of lead-free Sn-Zn-Bi alloys as a powerful radiation and neutron shielding material, Radiation physics and chemistry, **195** 110065.

18 Mohamed Saad, Hussain ALMohiy, Mohammed S. Alqahtani, Abdulaziz A. Alshihri & Rizk Mostafa Shalaby, (2022) Study of structural, physical, characteristics and radiation shielding parameters of Bi50-Pb40-Sn10 and Bi40-Pb40-Sn10-Cd10 alloys used for radiation therapy, Radiation effects & defects in solids, VOL. **177**, NOS. 5–6, 545–555 https://doi.org/10.1080/10420150.2022.2063125.

19 Rizk Mostafa Shalaby, Hussain Al-Mohiy, Mohammed S. Alqahtani, Abdulaziz A. Alshihri & Mohamed Saad, (2022) the influence of antimony additive on structural, mechanical, and nuclear radiation shielding parameters of rapidly quenched Pb-Sn binary alloy, Radiation effects & defects in solids, Published online: **11** Aug https://doi.org/10.1080/10420150.2022.2105216.

20 O. Mokhtari, H. Nishikawa, (2016) Correlation between microstructure and mechanical properties of Sn–Bi–X solders, Mater. Sci. Eng. A **651** 831–839.

21 Emin Çadırlı, Uğur Böyük, Hasan Kaya, Necmettin Maraşlı, (2011) Determination of mechanical, electrical and thermal properties of the Sn—Bi—Zn ternary alloy, *Journal of Non-Crystalline Solids*, **357** 2876-2881.

22 Shohreh Khorsand, Shouxun Ji, (2019) Electrochemical corrosion behaviour of Sn-Zn-xBi alloys used for miniature detonating cords Guangyu Liu, *Journal of Materials Science & Technology*, **35** 1618-1628.

23 M. Kamal, A.M. Shaban, M. El-Kady and R.M. Shalaby, (1996)." Irradiation, mechanical and structure behaviour of Aluminium-Zinc based alloys rapidly quenched from melt", Radiation Effects and Defects in Solids, OPA, Vol.**138**, pp.307-318.

24 M. Kamal, A.M. Shaban, M. El-Kady and R.M. Shalaby, (1994)." Determination of structure-property of rapidly quenched aluminium-based bearing alloys before and after gamma irradiation", 2nd International Conference of Engineering Physics and Mathematics, Faculty of Engineering, Cairo University, Cairo, Vol.**2**, pp.107-121.

25 C. Suryanarayana and T.R. Anantharaman, (1970). Solidification of aluminum– germanium alloys at high cooling rates, *J. Mat. Sci*. **5,** 992–1004

26 F. Hehmann, F. Sommer and B. Predel, (1990). Extension of solid solubility in magnesium by rapid solidification, Mat. Sci. Eng. A **125**, 249–265

27 R.M. Shalaby, (2009) influence of indium addition on structure, mechanical, thermal, and electrical properties of tin-antimony based metallic alloys quenched from melt, *J. Alloys Compd*. **480**, 334-339.

28 Nermin Ali Abdelhakim*, Rizk Mostafa Shalaby, Mustafa Kamal, (2018) A Study of Structure, Thermal and Mechanical Properties of Free Machining Al-Zn-Sn-Bi Alloys Rapidly Solidified from Molten State, *World Journal of Engineering and Technology*, , **6**, 637-650 http://www.scirp.org/journal/wjet.

29 Saad, G., Fayek, S.A., Fawzy, A., Soliman, H.N., Mohammed, G., (2010).

Deformation characteristics of Al-4043 alloy. Mater. Sci. Eng., A **527**, 904–910.
30 B.D.Cullity (1978), elements of X-ray diffraction, 2nd Edition(Addison-Wesely, , p.248.
31 B.D.Cullity, ,(1959) elements of X-ray diffraction, 2nd Edition, USA, , p.317,ch.10.
32 G.E. Dieter, D.J. Bacon, D. Bacon, (1988) Mechanical metallurgy (McGraw-Hill, New York,.
33 R.M.Shalaby (2012),, Effect of silicon addition on mechanical and electrical properties of Sn–Zn based alloys rapidly quenched from melt, Materials Science and Engineering: A, Volume **550**, 30 July Pages 112-117